Metal Nanostructures

DOI: 10.1002/anie.200905070

Template-Directed Synthesis of Nanoplasmonic Arrays by Intracrystalline Metalization of Cross-Linked Lysozyme Crystals**

*Mina Guli, Elizabeth M. Lambert, Mei Li, and Stephen Mann**

Many protein crystals are distinguished by 3-D structures that contain well-ordered interpenetrating nanoporous and mesoporous solvent channels often 0.5–10 nm in diameter.[1] These channels provide a chemically heterogeneous and chiral environment that comprises 30–65 % of the total crystal volume with associated pore volumes and surface areas in the range of 0.9–3.6 $mL\,g^{-1}$ and 800–3000 $m^2\,g^{-1}$, respectively.[1–3] The use of protein crystals for materials applications has been traditionally restricted by their mechanical and chemical fragility; however the onset of simple cross-linking technology has significantly extended the scope for protein aggregates and crystals in catalysis and drug delivery,[4,5] separation science,[2,6–8] and sensors.[9] In general, cross-linking is achieved by soaking the protein crystals in a 1–5 % aqueous glutaraldehyde solution containing a heterogeneous mixture of monomers and aldol-based oligomers of various lengths.[10] Reaction of these species with lysine residues results in a network of Schiff-base coupled intermolecular linkages to produce cross-linked protein crystals with high structural fidelity.[11] As a result, the glutaraldehyde-fixed crystals are physically robust, stable in organic solvents, and insoluble in water. Moreover, immersion of the cross-linked crystals in aqueous solutions of organic dyes, drugs, and antibiotics results in uptake of the guest molecules specifically within the solvent channels of the protein lattice.[12–16]

Here, we extend the above strategies for the sequestration of metal ions and their reduction products within the solvent channels of glutaraldehyde cross-linked lysozyme single crystals. We note that a related approach, but involving cross-linked virus crystals, has been used recently to template the deposition of Pt/Pd nanoparticles.[17] Lysozyme is an enzyme with a single polypeptide chain consisting of 129 amino acids ($M_w = 14600$), and can be readily crystalized in various polymorphic forms.[18–22] Significantly, the tetragonal polymorph (space group $P4_32_12$) has discrete uni-directional solvent channels, 1 to 2.5 nm in diameter, which are aligned parallel to the crystallographic c axis.[23] Each channel is located in the centre of the unit cell, surrounded locally by four protein molecules, and constructed from an interlinked network of pores and cavities lined with aspartate and lysine residues.[24] Herein, we exploit this structural arrangement as an ordered 1-D intracrystalline reaction environment for the periodic organization and nanoscale confinement of plasmonic nanowires of Ag or Au. Arrays of metallic nanofilaments are produced within the protein crystals by in situ redox reactions involving photoreduction of sequestered Ag^I ions or chemical reduction of $AuCl_4^-$ by BH_4^- ions pre-organized into the solvent channels. The resulting metalized protein crystals are physically robust, regular in external morphology, and uniform in size. Such materials represent a new class of hybrid monoliths with patterned nanostructured interiors, and may find uses as waveguides, sensors, and catalysts.

Native lysozyme crystals were grown and cross-linked with glutaraldehyde according to established methods.[25–27] Both the native and cross-linked crystals were uniform in size, 50–100 × 100–200 μm in dimension depending on the conditions of growth, and tetragonal prismatic in morphology. The cross-linked crystals were pale yellow in color, smoother in surface texture than the colorless native crystals, and comprised four relatively large {110} side faces capped by four inclined end faces of {101} form (Figure 1 a,b).[28] Soaking the cross-linked protein crystals in $AgNO_3$ solution in the dark for 3 days, followed by UV-induced photoreduction resulted in intact red-brown crystals (Figure 1 c) that contained approximately 10 wt % Ag (thermogravimetric analysis; see Supporting Information, Figure S1a). No changes in crystal size, morphology, or texture were observed after intracrystalline sequestration or photoreduction of the Ag^I ions (Figure 1 d). Similarly, no differences were apparent when cross-linked lysozyme crystals containing sequestered sodium borohydride were immersed in an aqueous $AuCl_4^-$ solution and left for 3 days (Figure 1 e,f), even though the crystals consisted of 23 wt % Au (Figure S1b). In both cases, energy dispersive X-ray (EDX) analysis and mapping of fractured crystals mounted onto scanning electron microscopy (SEM) stubs indicated penetration of Ag or Au into the protein crystal interior.

Single crystal X-ray diffraction studies on the native and cross-linked lysozyme crystals showed well ordered patterns that were indexed to a tetragonal unit cell ($\alpha = \beta = \gamma = 90°$) with unit cell parameters, a ($= b$) and c, of 7.74 and 3.73 nm, or 7.88 and 3.68 nm, respectively (Figure S2a,b). The observed expansion (1.8 %) and contraction (1.4 %) in the a and c axes, respectively, was in agreement with previous structural reports on glutaraldehyde-fixed lysozyme crystals,[11] and

[*] M. Guli, E. M. Lambert, Dr. M. Li, Prof. S. Mann
Centre for Organized Matter Chemistry, School of Chemistry
University of Bristol, Bristol BS8 1TS (UK)
E-mail: s.mann@bristol.ac.uk
Homepage: http://www.chm.bris.ac.uk/inorg/mann/webpage.htm
M. Guli
Department of Material Science and Engineering, Key Laboratory of Automobile Materials of Ministry of Education, Jilin University, Changchun, 130012 (P.R. China)

[**] This work was supported by the EPSRC (UK) and a grant from the China Scholarship Council. We thank Dr. Mairi Haddow for assistance with single crystal X-ray diffraction and Jonathan Jones for help with electron microscopy.

Supporting information for this article is available on the WWW under http://dx.doi.org/10.1002/anie.200905070.

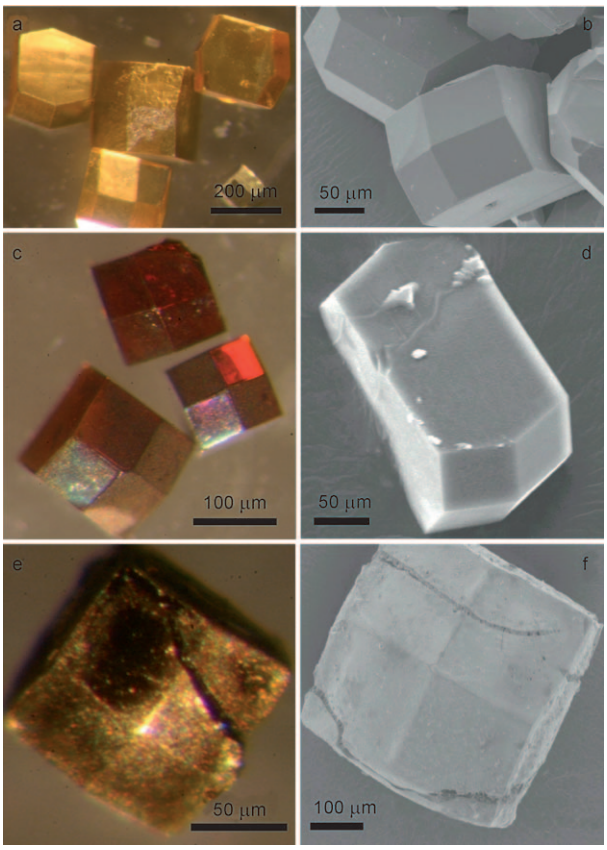

Figure 1. Optical and corresponding SEM micrographs for a,b) glutaraldehyde cross-linked lysozyme crystals; c,d) Ag-doped cross-linked lysozyme crystals after UV irradiation; and e,f) sodium borohydride-containing cross-linked lysozyme crystals after reaction with $AuCl_4^-$ ions.

was attributed to the formation of intermolecular cross-links preferentially along the lysine-rich walls of the solvent channels. Corresponding structural studies of the cross-linked Ag^I-doped protein crystals prior to photoreduction indicated no significant change in crystallographic structure. Although the intensities were somewhat reduced, the diffraction patterns were readily indexed to a tetragonal unit cell with parameters of $a = b = 7.88$ nm, $c = 3.61$ nm, and $\alpha = \beta = \gamma = 90°$ (Figure S2c). The data indicated that Ag^I binding in the solvent channels produced no change in the a axis parameter but caused a further 1.9% contraction along the c axis. In contrast, exposure of the Ag^I-containing lysozyme crystals to UV radiation for 10, 30, 60, or 360 min resulted in a progressive deterioration in the quality of the diffraction patterns. As some partial degradation of the control crystals was also observed during UV irradiation, we attributed the changes in the quality of the Ag-doped protein crystals to a combination of radiation damage and formation of Ag^0 species in the solvent channels. The latter was consistent with X-ray protein crystallography studies of cross-linked lysozyme crystals containing chemically reduced $AuCl_4^-$ ions, which showed only low intensity reflections that were provisionally indexed to a disordered tetragonal phase ($a = 7.23$, $b = 7.39$, $c = 3.32$ nm; $\alpha = 89.5$, $\beta = 88.5$, $\gamma = 87.5°$; Figure S2d). The above results were consistent with observations based on small angle X-ray diffraction (SAXRD) profiles of the native, cross-linked and metalized cross-linked lysozyme crystals (Figure S3).

Fourier transform infra-red (FTIR) spectra of the metalized lysozyme crystals remained effectively unchanged when compared with those for the native or cross-linked crystals (Figure 2a). In each case, bands corresponding to the protein

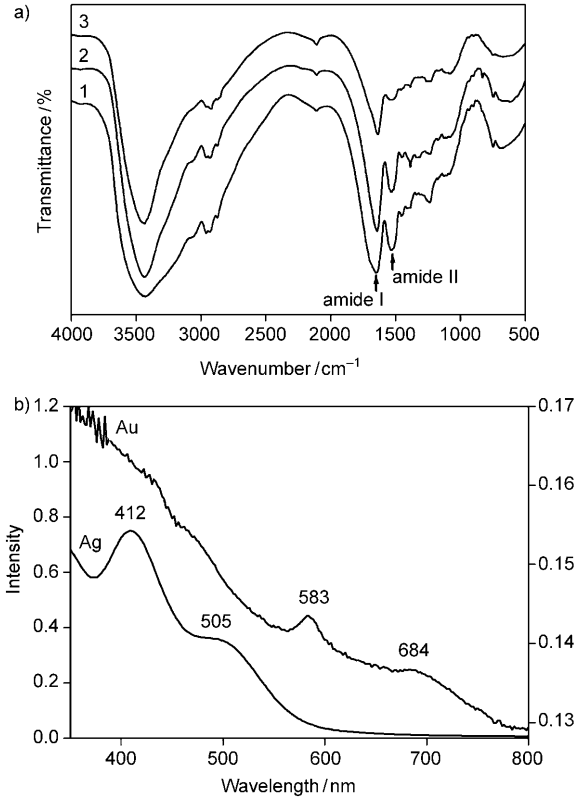

Figure 2. a) FTIR spectra of cross-linked lysozyme crystals; 1) as prepared, 2) Ag-doped, and 3) Au-doped. Arrows show amide I and II bands. b) Diffuse reflectance UV/Vis spectra for cross-linked single crystals of lysozyme after Ag or Au metalization.

amide I (C=O stretch, 1654 cm^{-1}), amide II (N–H in plane bend/C–N stretch, 1533 cm^{-1}) and amide III (1235 cm^{-1}) absorbances, along with the C–H symmetric and antisymmetric modes (2928 cm^{-1} and 2862 cm^{-1}, respectively), and C–H (methylene scissor, 1454 cm^{-1}) vibrations were observed. Significantly, diffuse reflectance UV/Vis spectra of the photoreduced Ag-doped lysozyme crystals showed transverse and longitudinal plasmon resonance peaks, typically at around 412 and 505 nm, respectively (Figure 2b). Similarly, two absorbance bands at 583 and 684 nm, corresponding to the transverse and longitudinal plasmon resonance peaks, respectively, for metallic gold were observed in the diffuse reflectance UV/Vis spectra of cross-linked protein crystals after in situ chemical reduction (Figure 2b). The data were consistent with previous reports on the plasmonic behavior of Ag and Au nanostructures,[29–32] and indicated that in both cases metallic nanostructures with high shape anisotropy were templated within the cross-linked lysozyme crystals.

The presence of an anisotropic metallic nanophase within the cross-linked lysozyme crystals was confirmed by high resolution transmission electron microscopy (HRTEM) of thin fragments of single crystals. Significantly, lattice images of the photoreduced Ag-containing crystals or chemically reduced Au-doped samples showed in both cases distinct electron dense stripes that were continuous over regions of several 100 nm^2 (Figure 3a,b). No such images were observed

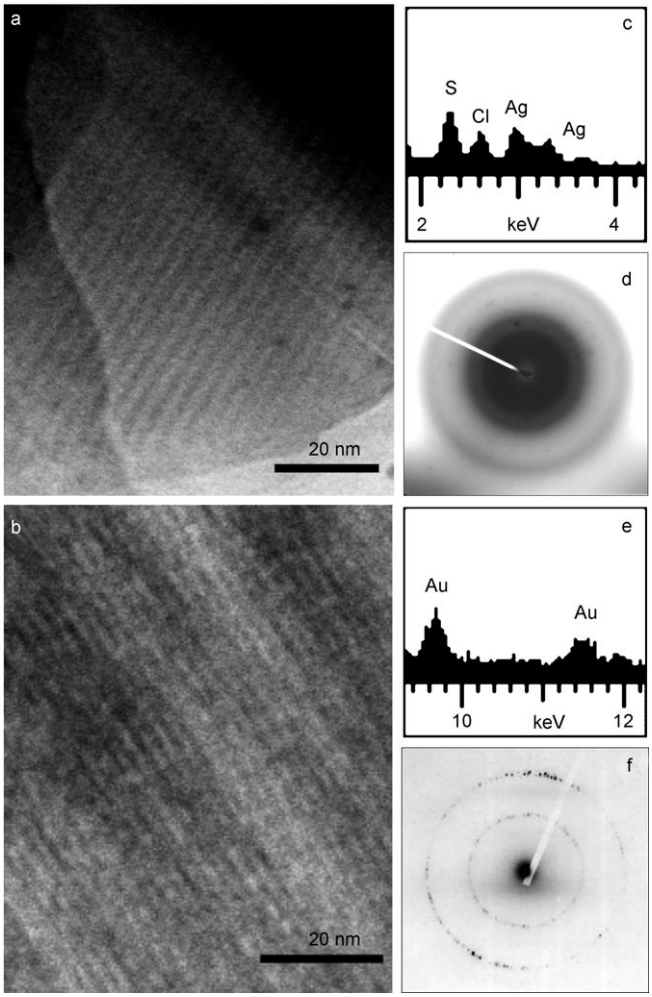

Figure 3. TEM images showing electron dense metallic nanofilaments for a) photoreduced Ag-doped cross-linked lysozyme crystals, and b) chemically reduced Au-containing cross-linked lysozyme crystals. Corresponding EDX analysis and electron diffraction data are shown in (c,d) and (e,f), respectively.

for the cross-linked protein crystals prior to photoreduction of the Ag-doped samples, or in the absence of Ag or Au ions. The average thicknesses of the electron dense stripes were 1.6 and 1.5 nm for the Ag and Au-loaded protein crystals, respectively (Figure S4), which were commensurate with the size of the solvent channels of the tetragonal lattice. Corresponding EDX analyses revealed peaks for Ag (3.0, 3.3, and 3.7 keV) or Au (9.7 and 11.5 keV; Figure 3c,e), along with an S peak at 2.3 keV from the protein molecules. Significantly, electron diffraction patterns showed low intensity, often incomplete rings corresponding to the (200) (0.204 nm), (220) (0.145 nm), and (311) (0.123 nm) planes of face-centred cubic (fcc) metallic Ag (Fm3m, $a = 0.4086$ nm), or the (200) (0.203 nm) and (222) (0.117 nm) reflections of fcc metallic Au (*Fm3m*, $a = 0.4064$ nm; Figure 3d,f). The above results clearly indicated that highly elongated Ag or Au nanostructures were confined specifically within the channels of the cross-linked lysozyme single crystals.

In conclusion, our results indicate that the deposition of periodically arranged Ag or Au nanostructures can be achieved by containment of redox reactions within the solvent channels of cross-linked lysozyme crystals. Lysozyme is inexpensive, commonly available and easy to crystallize, indicating that high yields and scale-up procedures should be possible. Moreover, the ability to crystallize lysozyme in various polymorphic forms provides an opportunity to tailor the architecture of the metalized nanostructures through judicious choice of the protein lattice. In this regard, intracrystalline metalization of the tetragonal lattice results in regular arrays of discrete protein-embedded nanoplasmonic filaments oriented specifically along the crystallographic *c* axis to produce macroscopic hybrid materials that should exhibit highly anisotropic properties. As the metalized protein crystals can be readily handled and physically manipulated it might be possible to integrate them as addressable components within optical, sensing, or catalytic devices. Finally, as the method is facile and highly reproducible it should be possible to develop the above strategies to prepare nanostructured arrays of many different types of functional inorganic or organic nanostructures. Such objectives will be explored in future work in our laboratory.

Experimental Section

Protein crystal growth and cross-linking: All chemicals were purchased from Sigma Aldrich. Water with a resistivity of 18 $\Omega\,cm^{-1}$ was used in all experiments, and all solutions were filtered before use through a 45 μm syringe filter. In a typical experiment, batch crystallization was performed using 24-well microtiter Rotilab plates (Carl Roth GmbH, Karlsruhe, Germany) at room temperature. Each well was filled with 2 mL of a solution containing 30 $mg\,mL^{-1}$ lysozyme and 60 $mg\,mL^{-1}$ NaCl in a 0.1M NaOAc buffer at pH 4.0. The plates were then sealed and aged for 24 h to produce well-formed tetragonal lysozyme crystals. Following crystalization, the reservoir solution was removed and replaced with 1 mL of a cross-linking solution which comprised 1% glutaraldehyde, 8% wt/vol NaCl and 0.05% NaN_3 in 0.1M NaOAc buffer at pH 4.0. The wells were resealed and the system left to stand for 2 h followed by shaking at 300 rpm for about 24 h. The cross-linking solution was subsequently removed to extract any small lysozyme aggregates, and the crystals washed with shaking 6 times. The stability of the cross-linked lysozyme crystals was established by maintaining a batch in water for about a week.

Metalization: Washed and dried cross-linked lysozyme crystals were soaked in solutions of silver nitrate (10^{-3} to 10^{-5} M, pH 6.6–7.5) for about three days in the dark at room temperature. The Ag-doped crystals were then washed in the dark at room temperature and then exposed at room temperature for up to 6 h to UV radiation using a lamp set at a wavelength of 254 nm. The photoreduced crystals were then collected and used directly for analysis. To prepare Au-containing crystals, washed and dried cross-linked lysozyme crystals were soaked in $NaBH_4$ (10^{-5} M, pH 8.9–9.5) at room temperature for 5 min, washed with water, and then dried at room temperature in a

vacuum oven. Intracrystalline metalization was then undertaken by soaking the borohydride-containing crystals in $HAuCl_4 \cdot 3H_2O$ (10^{-5} M, pH 3.9–4.2) solution for 3 days. The resulting crystals were washed and used for analysis.

Characterization procedures: see Supporting Information.

Received: September 10, 2009
Published online: December 10, 2009

Keywords: gold · hybrid materials · metal nanoparticles · protein crystals · silver

[1] B. W. Matthews, *J. Mol. Biol.* **1968**, *33*, 491 – 497.
[2] L. Z. Vilenchik, J. P. Griffith, N. St. Clair, M. A. Navia, A. L. Margolin, *J. Am. Chem. Soc.* **1998**, *120*, 4290 – 4294.
[3] V. N. Morozov, G. S. Kachalova, V. U. Evtodienko, N. F. Lanina, T. Y. Morozova, *Eur. Biophys. J.* **1995**, *24*, 93 – 98.
[4] A. L. Margolin, M. A. Navia, *Angew. Chem.* **2001**, *113*, 2262 – 2281; *Angew. Chem. Int. Ed.* **2001**, *40*, 2204 – 2222.
[5] A. L. Margolin, *Trends Biotechnol.* **1996**, *14*, 223 – 230.
[6] O. Pastinen, K. Visuri, M. Leisola, *Biotechnol. Tech.* **1998**, *12*, 557 – 560.
[7] O. Pastinen, J. Jokela, T. Eerikäinen, T. Schwabe, M. Leisola, *Enzyme Microb. Technol.* **2000**, *26*, 550 – 558.
[8] X. S. Peng, J. Jin, Y. Nakamura, T. Ohno, I. Ichinose, *Nat. Nanotechnol.* **2009**, *4*, 353 – 357.
[9] N. S. Wickremasinghe, J. H. Hafner, *Nano Lett.* **2005**, *5*, 2418 – 2421.
[10] H. K. Purss, G. C. Qiao, D. H. Soloman, *J. Appl. Polym. Sci.* **2005**, *96*, 780 – 792.
[11] Y. Wine, N. Cohen-Hadar, A. Freeman, F. Frolow, *Biotechnol. Bioeng.* **2007**, *98*, 711 – 718 (Protein Data Bank (PDB)-2HTX) http://www.rcsb.org/pdb/explore/explore.do?structureId = 2HTX.
[12] A. Cvetkovic, A. J. J. Straathof, *Langmuir* **2005**, *21*, 1475 – 1480.
[13] M. Subramanian, M. P. Venkatappa, *Curr. Sci.* **1982**, *51*, 778 – 780.
[14] M. Subramanian, B. S. Sheshadri, M. P. Venkatappa, *J. Biochem.* **1984**, *96*, 245 – 252.
[15] J. R. Wendorf, C. J. Radke, H. W. Blanch, *Biotechnol. Bioeng.* **2004**, *87*, 565 – 573.
[16] A. Cvetkovic, A. J. J. Straathof, L. A. M. Van der Wielen, *Biotechnol. Bioeng.* **2004**, *86*, 389 – 398.
[17] J. C. Falkner, M. E. Turner, V. L. Colvin, *J. Am. Chem. Soc.* **2005**, *127*, 5274 – 5275.
[18] C. Sauter, F. Otalora, J. A. Gavira, O. Vidal, R. Giege, J. M. Garcia-Ruiz, *Acta Crystallogr. Sect. D* **2001**, *57*, 1119 – 1126.
[19] S. Saijo, Y. Yamada, T. Sato, N. Tanaka, T. Matsui, G. Sazaki, K. Nakajima, Y. Matsuura, *Acta Crystallogr. Sect. D* **2005**, *61*, 207 – 217.
[20] K. Harata, T. Akiba, *Acta Crystallogr. Sect. D* **2006**, *62*, 375 – 382.
[21] M. A. Walsh, T. R. Schneider, L. C. Sieker, Z. Dauter, V. S. Lamzin, K. S. Wilson, *Acta Crystallogr. Sect. D* **1998**, *54*, 522 – 546.
[22] C. Brinkmann, M. S. Weiss, E. Weckert, *Acta Crystallogr. Sect. D* **2006**, *62*, 349 – 355.
[23] J. C. Falkner, A. M. Al-Somali, J. J. Jamison, J. Zhang, S. L. Adrianse, R. L. Simpson, M. K. Calabretta, W. Radding, G. N. Phillips, V. L. Colvin, *Chem. Mater.* **2005**, *17*, 2679 – 2686.
[24] Z. Hu, J. Jiang, *J. Membr. Sci.* **2008**, *324*, 192 – 197.
[25] D. Hekmat, D. Hebel, H. Schmid, D. Weuster-Botz, *Process Biochem.* **2007**, *42*, 1649 – 1654.
[26] R. A. Judge, E. L. Forsythe, M. L. Pusey, *Biotechnol. Bioeng.* **1998**, *59*, 776 – 785.
[27] Q. Huang, Z. Wang, G. Zhu, M. Qian, M. Shao, Y. Jia, Y. Tang, *Biochim. Biophys. Acta* **1998**, *1384*, 335 – 344.
[28] M. C. R. Heijna, W. J. P. van Enckevort, E. Vlieg, *Cryst. Growth Des.* **2008**, *8*, 270 – 274.
[29] K. Esumi, K. Torigoe, *Prog. Colloid Polym. Sci.* **2001**, *117*, 80 – 87.
[30] C. Petit, P. Lixion, M. P. Pileni, *J. Phys. Chem.* **1993**, *97*, 12974 – 12983.
[31] T. Saraidarov, V. Levchenko, I. Popov, R. Reisfeld, *Superlattices Microstruct.* **2009**, *46*, 171 – 175.
[32] S. Lin, M. Li, E. Dujardin, C. Girard, S. Mann, *Adv. Mater.* **2005**, *17*, 2553 – 2559.

